

Global Solar Radiation Prediction Methodology using Artificial Neural Networks for Photovoltaic Power Generation Systems

Jane Oktavia Kamadinata¹, Tan Lit Ken¹ and Tohru Suwa²

¹Takasago Thermal/Environmental Systems Laboratory, Malaysia-Japan International Institute of Technology, Universiti Teknologi Malaysia, Kuala Lumpur, Malaysia

²Department of Mechanical Engineering, President University, Cikarang, Bekasi, Indonesia

Keywords: Artificial Neural Network, Global Solar Radiation Prediction, Sky Image, Photovoltaic Power Generation.

Abstract: Solar radiation is an essential source of energy that has yet to be fully utilized. This energy can be converted into another form of more usable energy, electricity, by using photovoltaic power generation systems in order to fight against global warming. When the photovoltaic power generation systems are connected to an electrical grid, predicting near-future global solar radiation is important to stabilize the entire network. Two different simple methodologies utilizing artificial neural networks (ANNs) to predict the global solar radiation in 1 to 5 minutes in advance from sky images are developed and compared. In the first methodology, two ANNs are combined. The first ANN predicts cloud movement direction, while the second ANN predicts global solar radiation using the first ANN's prediction results. On the other hand, a single ANN directly predicts global solar radiation in the second methodology. Both of the proposed methodologies are able to capture the trends of the global solar radiation well. Because the proposed methodologies only use limited number of sampling points, the computational effort is significantly reduced compared to the existing methodologies where the whole images need processing.

1 INTRODUCTION

Photovoltaic is one of the most promising renewable technologies for decelerating global warming. The global solar radiation, which is used by photovoltaic cells, tends to fluctuate. Due to the uncertainty of global solar radiation, its prediction methodology is needed in order to stabilize the entire electrical grid. When the total electricity provided by photovoltaic power generation systems to the electrical grid is significant, balancing the supply and demand is a critical issue because of the fluctuation. Usually multiple conventional power generation plants, which can be thermal, nuclear, or hydroelectricity, are connected to the electrical grid beside the photovoltaic power generation systems. The electricity is provided by the multiple conventional power plants so that the supply is balanced with the load. If a large fluctuation occurs in the electricity provided by the photovoltaic power generation systems, an extra power plant may have to start or shut down to compensate the disturbance. In such situations, the global solar radiation prediction

results in a few minutes in advance are useful to operate the electrical grid with the power plants.

For the past few years, various global solar radiation prediction methodologies have been proposed. Meteorological data along with geographical information is frequently used for predicting global solar radiation. Sunshine duration, relative humidity, and air temperature data have been used as the inputs for artificial neural network (ANN) to predict hourly global, diffuse, and direct solar irradiance (Mellit et al., 2010). Month, day, hour, temperature, and relative humidity data (Hasni et al., 2012), and a combination of monthly mean daily sum satellite-estimated data with latitude, longitude, and altitude information (Şenkal, 2010) have been used to predict global solar radiation. The predictions that use complete meteorological data provide good accuracy. However, since the past complete meteorological data is not available for most of the locations, above methodologies are useful in limited situations.

Other popular techniques to predict solar radiation are sky image-based methodologies. Most of these prediction methodologies focus on cloud

detection and tracking since solar radiation is highly affected by clouds. Short-term predictions for all of the solar radiation components (global, direct, and diffuse) have been performed by detecting cloud motion vectors from sky images taken by a total sky imager (Alonso-Montesinos et al., 2015, Marquez and Coimbra, 2013). Representative velocities and grid cloud fractions are used to predict direct solar radiation (Marquez and Coimbra, 2013). A machine learning algorithm combined with local irradiance data and sky images are used to forecast global and direct solar radiation (Pedro and Coimbra, 2015). A hybrid of ANN and support vector machine is used to produce prediction interval for direct solar radiation forecast (Chu et al., 2015). One of the major advantages of the prediction methodologies based on sky images is that they do not need complete meteorological data, which requires expensive measurement systems. For smaller photovoltaic power generation systems, it is not practical to have such systems. However, sky image-based methodologies require large computational effort in order to process multiple sky images as hundreds of thousands of pixels are contained in a single image.

In this work, two methodologies to predict global solar radiation in 1 to 5 minutes in advance by using measured global solar radiation, and sky images are proposed. In order to achieve accurate and fast prediction, ANNs are used in these methodologies. Unlike most of the sky image-based prediction methodologies, the proposed methodologies process image information obtained from less than fifty pixels in each image, resulting in much less computational effort. The proposed methodologies do not require meteorological data such as humidity or air temperature. Hence they are suitable for areas where the complete weather measurement system is not available.

2 GLOBAL SOLAR RADIATION PREDICTION METHODOLOGIES

In this paper, two solar radiation prediction methodologies using ANNs with sky images are proposed. The first proposed methodology, 2-step method, consists of 2 ANNs. In this methodology, image information from sampling points is extracted from the sky images. Then, the extracted image information is used as the inputs for the first ANN to predict the direction of cloud movement. Lastly, the

image information from sampling points close to the predicted cloud movement direction combined with measured global solar radiation values are used as the inputs for the second ANN to predict solar radiation in 1 to 5 minutes in advance. The second proposed methodology, 1-step method uses only one ANN. In this methodology, sky image information extracted from the sampling points is combined with the measured global solar radiation data as the inputs for the ANN to directly predict global solar radiation in 1 to 5 minutes in advance. The predicted results are compared with the measured global solar radiation data using root mean square error (RMSE):

$$RMSE = \sqrt{\frac{\sum_{i=1}^n (v_{p,i} - v_{m,i})^2}{n}} \quad (1)$$

where $v_{p,i}$ is the predicted global solar radiation value in W/m^2 , $v_{m,i}$ is the measured global solar radiation value in W/m^2 and n is the number of times to perform prediction. The subscript i denotes the ANN testing data set number.

2.1 Prediction using Artificial Neural Networks

ANN has been proven to be suitable for solar radiation prediction when meteorological and geographical data are used as the inputs. In this research, commercially available artificial neural network software (Ward System Groups, 1996) is used to predict global solar radiation. The general configuration of the artificial neural network is illustrated in Figure 1. The rectangles in hidden layer represent groups of neurons. The input, hidden layer, and output neurons are fully connected.

Each of the rectangles in the hidden layer has its own activation function. From preliminary analysis, four activation functions are chosen to form the rectangles: Gaussian, Gaussian complement, hyperbolic tangent (Tanh), and jump connection. The formula of the Gaussian activation function is described as (Ward System Groups, 1996) :

$$f(x) = e^{-x^2} \quad (2)$$

The Gaussian complement activation function is described as (Ward System Groups, 1996):

$$f(x) = 1 - e^{-x^2} \quad (3)$$

The hyperbolic tangent activation function is described as (Ward System Groups, 1996):

$$f(x) = \tanh(x) \quad (4)$$

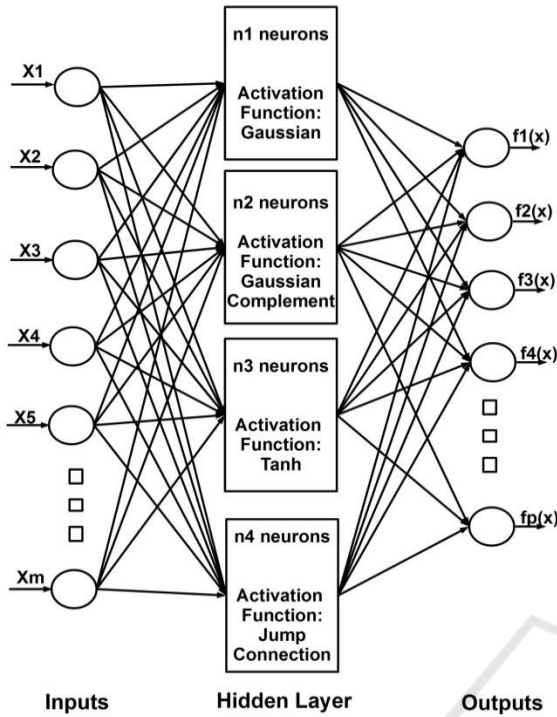


Figure 1: Artificial neural network configuration.

Jump connection activation function is described as:

$$f(x) = x \quad (5)$$

In the preliminary analysis, the best network activation function combination, which minimizes the RMSE, is selected from all of the possible 2 to 4 activation function combinations. At the same time, parameters for artificial neural network learning process: number of neurons in the rectangles, learning rate, momentum, and initial weights, are optimized so that the RMSE is minimized. The parameters called learning rate and momentum control how the weights are modified in the next iteration within the network learning process. The initial weights are randomly selected numbers within a specified range. It is confirmed that initial weights within the range from -0.3 to 0.3 result in the most accurate prediction for most of the networks. As a result, each artificial network consists of different activation function combination with different number of neurons in the rectangles.

The number of neurons in a rectangle, n_n , is decided by the next equation (Ward System Groups, 1996):

$$n_n = \frac{n_i - n_o}{2} + \sqrt{n_t} \quad (6)$$

where n_i is the number of ANN inputs, n_o is the number of outputs, and n_t is the number of training data sets. Equation 6 applies to all of the hidden layer rectangles except for the rectangle with jump connection whose number of neurons is the same as number of inputs, which is described as:

$$n_n = m \quad (7)$$

where m is the number of input neurons.

In the preliminary analysis, it is confirmed the number of neurons obtained from these equations give the most accurate prediction results.

2.2 Data Collection

The sky images are taken using a waterproof 12-megapixel camera with a fish-eye lens mounted on a 2-axis solar tracker. In front of the camera, the sun is covered by a circular shade so that direct sunlight does not reach to the lens to avoid glares. The sky images are taken with 20-second intervals.

The second data used in this research are the global solar radiation data. Minutely global solar radiation data are measured with a pyranometer and taken simultaneously with the sky images. The pyranometer is located within 100 m from the camera to make sure that the sky images taken are relevant to the solar radiation measurement.

2.3 Image Information Extraction

Various image information extraction techniques such as the intensity, hue, and saturation color space (Souza-Echer et al., 2006), hue, saturation, and value (HSV) color space and red, green, blue (RGB) color space (Davis et al., 1991, Sabburg and Wong, 1999), the red blue ratio (RBR) (Chow et al., 2011), and normalized ratio of red intensity to blue intensity (nRBR) (Chu et al., 2015) have been proposed to distinguish clouds from the clear sky for cloud classification problems.

During the preliminary analysis, it is discovered that RBR values differentiate clouds from the blue sky effectively. The RBR is the ratio of red and blue values taken from a pixel. A RBR value in the blue sky shows lower values, while a higher value of RBR is obtained in clouds no matter how dark or bright. In this research, RBR values are extracted from sampling points at predetermined locations.

Five successive sky images taken with 20-second intervals are used for a set of ANN input data. The sampling points are placed so that they are radiated from the center of the sun. In every image, 4 axes are drawn towards the center of the sun, as shown in

Figure 2a. On every line, 5 sampling points are placed with the same intervals of 1.86° . Although a fisheye lens is used to capture the sky images, it is confirmed the image distortion is negligible in the area where the sampling points are located. RBR values from the sampling point are then extracted and used as the ANNs inputs as described in Section 2.4 and Section 2.5. In Figure 2a, the direction of cloud movement is expressed as a number from 1 to 5, denoted by the axes from D1 to D5. D1 is used twice to include the area between D4 and D1.

Assuming cloud movement toward the sun is the most critical information for predicting global solar radiation, the RBR value sampling points are located so that they are radiated from the center of the sun. In an image, there are 5 points located on each axis line, resulting in a total of 20 sampling points. In 5 images, there are 100 sampling points in total. In order to obtain the relation between the number of the sampling points and prediction accuracy, 6 and 8-axis cases are also used for the prediction. In the cases of 6 and 8-axes, there are total sampling points of 150 and 200 as shown in Figure 2b and Figure 2c, respectively. In this section, the prediction methodology using 4-axes is discussed as an example. For 6 and 8-axes cases, the number of ANN inputs is increased as the number of sampling points increases.

A total of 1,580 sets equivalent to about 44 hours of measured solar radiation data and sky images are used for training the artificial neural networks. Among the 1,580 data sets, 80% is used for training the network, while the remaining 20% is for testing. In order to avoid overtraining, RMSE are calculated by using the measured data different from the ones used for network training during the testing process.

2.4 2-Step Method for Global Solar Radiation Prediction

2-step method consists of two ANNs: ANN 1 for step 1 and ANN 2 for step 2, as shown in Figure 3.

In the first step, a total of 100 RBR values extracted from the sampling points are used as the inputs of ANN 1 to predict cloud movement direction. In total, this ANN Step 1 uses 100 inputs to produce 1 output. The 6 and 8-axis cases have different number of inputs, still the number of output is always one: the cloud movement direction. The cloud movement direction used for training ANN 1 is obtained manually by comparing the consecutive sky images.

RBR values extracted from 5 points that fall in the line closest to the cloud movement direction predicted by ANN 1 are taken from every image. In the 5 images, a total of 25 points, added to 2 global solar radiation values measured at the corresponding time of the images taking process, are the inputs for ANN 2 to predict global solar radiation in 1 to 5 minutes in the future. In total, this ANN 2 will use 27 inputs to produce 5 outputs. Table 1 shows the ANN design for ANN step 1 and ANN step 2 for 4, 6, and 8 axes.

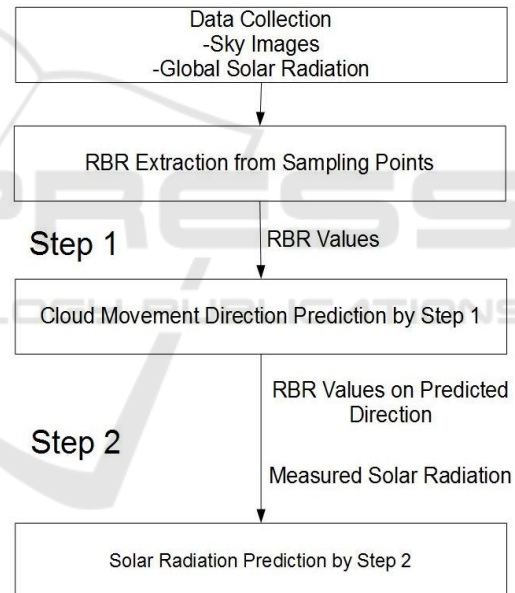


Figure 3: 2-step method for global solar radiation prediction.

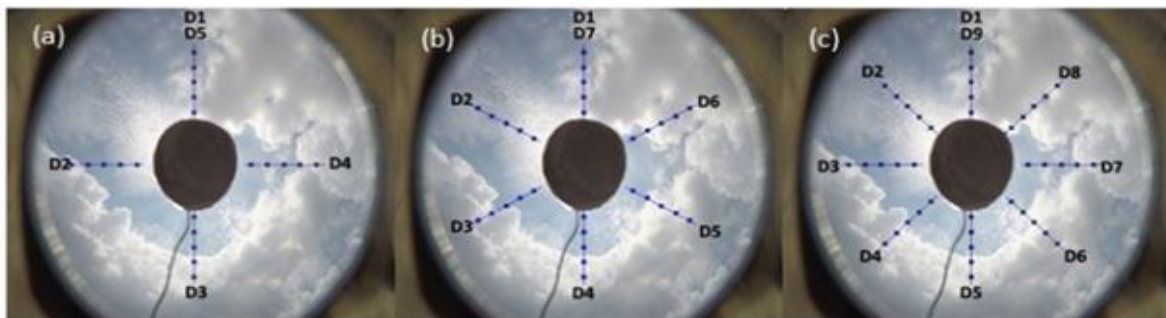


Figure 2: Image sampling points. (a) 4 Axes. (b) 6 Axes. (c) 8 Axes.

Table 1: 2-steps ANN design for 4, 6, and 8 axes.

Parameter	ANN Step 1			ANN Step 2		
	4 Axis	6 Axis	8 Axis	4 Axis	6 Axis	8 Axis
Number of hidden layer	3	3	3	2	3	3
Number of neurons in 1 hidden layer	27	35	44	24	16	24
Activation Function	Gaussian, Gaussian complement, Tanh	Gaussian, Gaussian complement, Tanh	Gaussian, Gaussian complement, Tanh	Gaussian, Gaussian complement	Gaussian, Gaussian complement, Tanh	Gaussian, Gaussian complement, Jump connection
Number of inputs	100	150	200	27	27	27
Number of outputs	1	1	1	5	5	5

2.5 1-Step Method for Global Solar Radiation Prediction

In 1-step method, the global solar radiation is directly predicted without predicting the cloud movement direction, as shown in Figure 4. The total of 100 RBR values extracted from the sampling points are combined with 2 global solar radiation values measured at the same time as the sky image taking process and used as the inputs for the ANN. In total, the 1-step method ANN has 102 inputs and gives 5 outputs, which are global solar radiation in 1 to 5 minutes in advance. The ANN design used for this methodology is listed in Table 2.

3 GLOBAL SOLAR RADIATION PREDICTION RESULTS AND DISCUSSIONS

In this section, solar radiation prediction results using 2-step and 1-step methods with three different numbers of axes are presented. The comparison of RMSE values of global solar radiation prediction in 1 to 5 minutes in advance with different prediction methods and different number of axes is shown in Figure 5. In order to avoid ANN overtraining, the prediction errors (RMSE) used in this work are calculated by using another measured data different from the ones used for network training. A total of 535 data sets, which are equivalent to about 15 hours, are used for RMSE calculations.

A smaller RMSE value indicates the predicted results are more accurate. The 6 and 8-axis cases of

Table 2: 1-steps ANN design for 4, 6, and 8 axes.

Parameter	1-Step ANN		
	4 Axis	6 Axis	8 Axis
Number of hidden layer	3	3	2
Number of neurons in 1 hidden layer	28	35	67
Activation Function	Gaussian, Gaussian Complement, Tanh	Gaussian, Gaussian Complement, Tanh	Gaussian, Gaussian Complement, Tanh
Number of inputs	102	152	202
Number of outputs	5	5	5

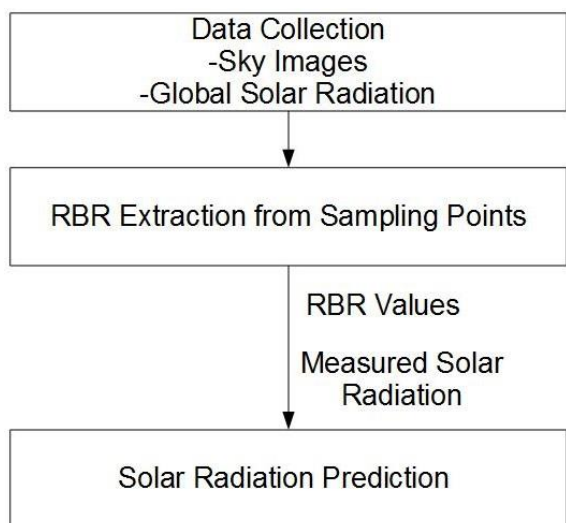


Figure 4: 1-step method for global solar radiation prediction.

2-step method gives more accurate results than 1-step method or 4-axis cases, although the differences are small. As the prediction minute increases, the accuracy tends to degrade. As originally expected, the accuracy is improved when the number of axes is increased but the difference is not large.

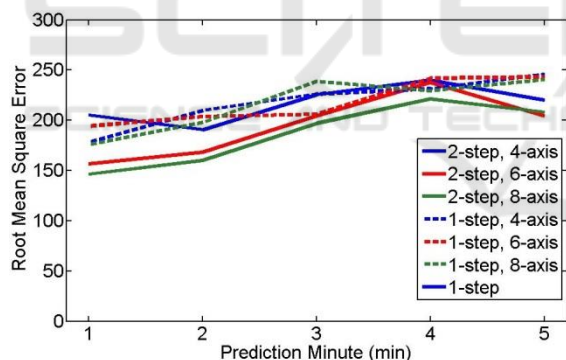


Figure 5: Comparison of RMSE values of 2-steps and 1-step methods.

At the same time, 4-axis cases give much better results than expected for both 2 and 1-step methods. Considering 4-axis cases use only 20 pixels per image, the accuracy of these results is rather surprising. The less axes cases require less sampling points and less data sets for ANN training. Therefore, at the training process requires less computational efforts at the cost of slightly less accuracy.

In Kuala Lumpur, there are many clouds in the sky quite often due to the high humidity. Because of these clouds, the solar radiation frequently increases

or decreases to a large extent. A typical day with fluctuating solar radiation value is chosen to demonstrate the capability of the proposed method. Figure 6 shows solar radiation prediction results of 1 minute in advance for 2-steps method, 6-axis case. Despite the small ups and downs, the proposed methodology captures the trend of solar radiation well. The proposed methodologies are especially good at predicting sudden large increases and decreases.

The cloud movement direction data is required for 2-step method for training ANN 1, while 1-step method does not need such data. Since the cloud movement direction is detected manually from the sky images, 1-step method has an advantage over 2-step for omitting this manual process. Also, 1-step method has simpler prediction process than 2-step.

Image information from hundreds of thousands of pixels is used for the existing cloud detection based solar radiation prediction methods, while only hundreds of pixels are used for the proposed methodologies. Because of this significant input data size reduction, much less computational efforts are needed for the proposed methods.

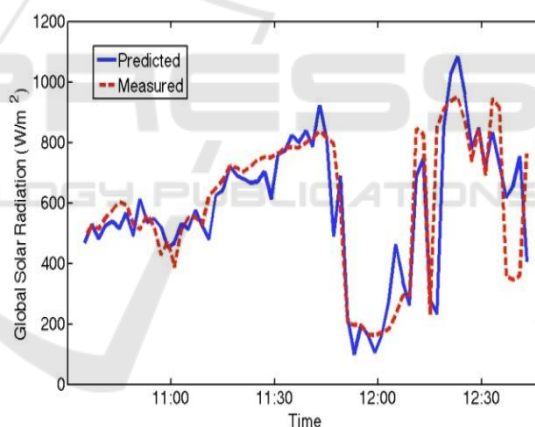


Figure 6: Global solar radiation prediction results compared to measured data, 1 minute in advance, 2-step, and 6-Axis. The data is measured on 28th July 2016.

In this example, the proposed methodology takes 5.4 seconds for the prediction on a personal computer with a 2.2 GHz quad-core processor and 8 GB memory. The prediction is performed for every 2 minutes during the daytime of July 28, 2016 equivalent to consecutive 2 hours and 8 minutes, which leads to 65 times of prediction as a total.

For most of the cloud detection methodologies in the previous work, sky imagers that are specially designed for taking sky images are required, while the proposed methodologies use a general-use waterproof camera, which is much less expensive

than the sky imagers. At the same time, the prediction can be performed by using commercially available ANN software. Software specifically developed for solar radiation prediction is not needed. A general use personal computer can be used for the prediction since the required computational efforts are limited. Because the proposed methodologies do not require special equipment, nor software, global solar radiation prediction is possible for much less cost compared to the existing methodologies.

The authors are currently improving the accuracy of prediction by optimizing the network configurations and their parameters. When an ANN has relatively large number of inputs, its prediction accuracy tends to be degraded. Having hundreds of inputs, the prediction accuracy may not be improved even if the number of axes is increased further.

4 CONCLUSIONS

Two different methodologies to predict global solar radiation in 1 to 5 minutes in advance using sky images are proposed. Image information extracted from a total of maximum 40 points placed in one image, combined with global solar radiation values measured simultaneously with the sky images photo taking, are used as the inputs for ANNs to predict global solar radiation values. The global solar radiation predicted by the proposed methodologies captures the trends of the measured data well even when there are sudden changes. When the number of sampling points is increased the prediction accuracy tends to be improved but the difference is rather small. The proposed 2-step method (6 and 8-axis) gives more accurate results than 1-step method but the difference is not large. Cloud movement direction data, which requires manual measurement, is needed for 2-step method, while 1-step method does not need it.

This methodology is focused on global solar radiation prediction in 1 to 5 minutes in advance because it is assumed that 1 to 5 minutes is enough for an electrical grid to prepare for output changes from a solar electricity generation system. The number of sampling points in the sky images, the sampling point interval, and the time interval to take the sky images are optimized for the 1 to 5 minutes prediction. It is expected that this methodology is applicable for predictions longer than 5 minutes when the data sampling parameters are optimized.

These proposed methodologies have an advantage of requiring much less computational

resources and efforts compared to the existing sky image-based prediction methodologies. These methodologies do not need complete meteorological data and suited to locations with no weather measurement systems.

ACKNOWLEDGEMENTS

The authors would like to express their appreciation to Takasago Thermal Engineering Co., Ltd. and Universiti Teknologi Malaysia for supporting this research through Takasago Research Grant Vot No. 4B211. The authors also wish to thank Wind Engineering for (Urban, Artificial, Man-made) Environment Lab (Dr. Sheikh Ahmad Zaki) in Malaysia-Japan International Institute of Technology for providing the global solar radiation data.

REFERENCES

- Alonso-Montesinos, J., Batlles, F.J., Portillo, C., 2015. Solar irradiance forecasting at one-minute intervals for different sky conditions using sky camera images. *Energy Convers. Manag.* 105, 1166–1177.
- Chow, C.W., Urquhart, B., Lave, M., Dominguez, A., Kleissl, J., Shields, J., Washom, B., 2011. Intra-hour forecasting with a total sky imager at the UC San Diego solar energy testbed. *Sol. Energy* 85, 2881–2893.
- Chu, Y., Li, M., Pedro, H.T.C., Coimbra, C.F.M., 2015. Real-time prediction intervals for intra-hour DNI forecasts. *Renew. Energy* 83, 234–244.
- Davis, G.B., Griggs, D.J., Sullivan, G.D., 1991. Automatic Estimation of Cloud Amount Using Computer Vision. *J. Atmos. Ocean. Technol.*
- Hasni, A., Sehli, A., Draoui, B., Bassou, A., Amieur, B., 2012. Estimating global solar radiation using artificial neural network and climate data in the south-western region of Algeria. *Energy Procedia* 18, 531–537.
- Marquez, R., Coimbra, C.F.M., 2013. Intra-hour DNI forecasting based on cloud tracking image analysis. *Sol. Energy* 91, 327–336.
- Mellit, A., Eleuch, H., Benghanem, M., Elaoun, C., Pavan, A.M., 2010. An adaptive model for predicting of global, direct and diffuse hourly solar irradiance. *Energy Convers. Manag.* 51, 771–782.
- Pedro, H.T.C., Coimbra, C.F.M., 2015. Nearest-neighbor methodology for prediction of intra-hour global horizontal and direct normal irradiances. *Renew. Energy* 80, 770–782.
- Sabburg, J., Wong, J., 1999. Evaluation of a ground-based sky camera system for use in surface irradiance measurement. *J. Atmos. Ocean. Technol.* 16, 752–759.

- Şenkal, O., 2010. Modeling of solar radiation using remote sensing and artificial neural network in Turkey. *Energy* 35, 4795–4801.
- Souza-Echer, M.P., Pereira, E.B., Bins, L.S., Andrade, M.A.R., 2006. A simple method for the assessment of the cloud cover state in high-latitude regions by a ground-based digital camera. *J. Atmos. Ocean. Technol.* 23, 437–447.
- Ward System Groups, 1996. NeuroSHELL 2 User Manual [WWW Document]. URL <http://www.wardsystems.com/manuals/neuroshell2/> (accessed 11.1.16).

